

A filter-flow perspective of hematogenous metastasis offers a non-genetic paradigm for personalized cancer therapy

Jacob G. Scott^{1,2}, Alexander G. Fletcher², Philip K. Maini², Alexander R.A. Anderson¹, & Philip Gerlee^{1,3}

¹ Integrated Mathematical Oncology, H. Lee Moffitt Cancer Center and Research Institute, Tampa, FL, USA

² Wolfson Centre for Mathematical Biology, Mathematical Institute, Radcliffe Observatory Quarter, Oxford University, Woodstock Road, Oxford OX2 6GG, UK

³ Mathematical Sciences, University of Gothenburg and Chalmers University of Technology, SE-41296 Gothenburg, Sweden

Prepublication draft.

Running title: filter-flow perspective

Keywords: metastasis, mathematical model, cancer, personalized medicine, oligometastasi

Correspondence:

Jacob G. Scott, jacob.g.scott@gmail.com and Philip Gerlee, gerlee@chalmers.se

Abstract

Research into mechanisms of hematogenous metastasis has largely become genetic in focus, attempting to understand the molecular basis of ‘seed-soil’ relationships. Preceding this biological mechanism is the physical process of dissemination of circulating tumour cells (CTCs). We utilize a ‘filter-flow’ paradigm to show that assumptions about CTC dynamics strongly affect metastatic efficiency: without data on CTC dynamics, any attempt to predict metastatic spread in individual patients is impossible.

Brief Communication

Nearly 150 years after Ashworth’s discovery of the vector of hematogenous metastatic disease, the circulating tumor cell (CTC) Ashworth [1869], the mechanisms driving this process remain poorly understood and unstoppable Plaks et al. [2013]. For over a century the dominant paradigm has been the seminal, yet qualitative, seed-soil hypothesis proposed by Paget in 1889 Paget [1989]. This began to be challenged in 1992, when a quantification of the contribution of mechanical and seed-soil effects was attempted by Weiss [Rapp, 2001], who considered the ‘metastatic efficiency index’ (MEI) of individual primary tumors and metastatic sites Weiss [1992]. He calculated MEI as the ratio of metastatic involvement to blood flow through an organ and three classes emerged: low, where the soil-organ relationship is hostile; high, where it is friendly; and medium, where blood flow patterns to a large extent explain patterns of spread. The utility of Weiss’ classification method largely ended there, and has since been put aside in favor of genetic correlations Minn et al. [2005], Bos et al. [2009]. While illuminating, this approach has yet to offer any actionable conclusions, and its applicability is threatened by the growing understanding that genetic heterogeneity, not clonality, is the rule in cancer Marusyk et al. [2012], Gerlinger et al. [2012].

We seek here to use Weiss’ MEI and a recently proposed model of CTC dynamics (summarised in Figure 1) Scott et al. [2012, 2013] to extend our understanding of metastasis. In so doing, we can explain, using a *translatable, patient parameter-specific method*, the population-level data for *any* given cancer. Our method also presents a way to utilize ‘personalized’ patient CTC measurements to assay for the burden and distribution of metastatic disease which can be used for guiding organ-directed therapy and more precise staging.

Until recently, even perfect information about the existence and distribution of metastatic disease would have done little to affect treatment choice, as the options were largely limited to the use of systemic chemotherapy. However, recent years have witnessed the advent of more effective localized therapies for metastatic involvement, in the form of liver-directed therapy, bone-seeking

radionuclides and stereotactic body radiation therapy. These novel modalities have allowed for targeted therapy to specific parts of the body with minimal side effects and high eradication potential. Further, trials offering treatment with curative intent to patients with limited, ‘oligometastatic’ disease have shown promise Milano et al. [2009, 2012], although it is not yet possible to identify such patients in an objective manner Weichselbaum and Hellman [2011].

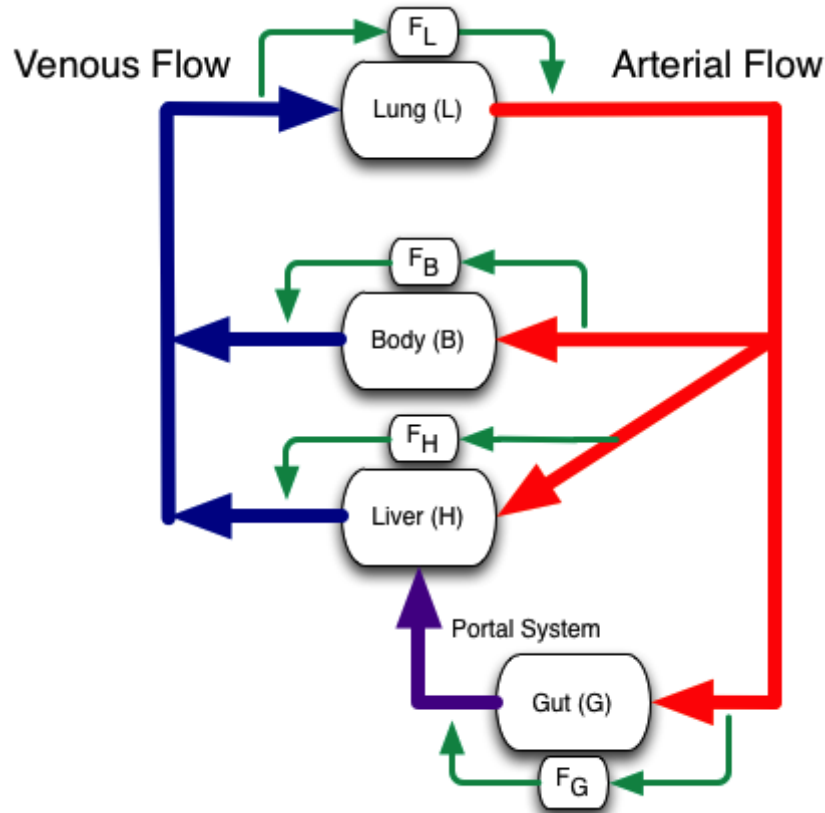


Figure 1: Schematic of the human vascular system network topology. It is evident by inspection of the network diagram that tumors originating in the gut and lung experience significantly different flow patterns and a different order in which they experience filtration at capillary beds than tumors originating in other parts of the ‘body’ [Scott et al., 2012]. The alternate pathways (green) represent the fraction of cells which evade arrest (filtration) at a given capillary bed. There are scant measurements of this fraction in the literature, and none in clinical studies that evaluate outcomes. We postulate that by ascertaining the distribution of CTCs in this network for individual patients, information about the existence of subclinical metastatic disease, and therefore metastatic propensity, will come to light, and allow for better staging, prognostication and rational use of organ-directed therapy in the setting of oligometastatic disease.

In this letter we extend Weiss’ method to understand metastatic proclivities of certain organ

sites and to provide a framework by which to understand the metastatic distribution from novel CTC measurements. To do this, we consider blood flow between organs Williams and Leggett [1989], filtration in capillary beds (see Figure 1 and Table 1) and distribution of metastatic involvement in a series of untreated patients at autopsy Disibio and French [2008]. For each organ-organ pair we calculate the MEI by normalising incidence by putative CTC flow between the two organs, taking into account the reduction that occurs in capillary beds Scott et al. [2012, 2013]; which has been shown to be of the order of 10^{-4} cell⁻¹ Okumura et al. [2009]. This post-capillary bed reduction in CTC numbers can be altered by the presence of micrometastases, which can amplify CTC numbers downstream of their location through shedding. Thus, by adjusting filtration rates throughout the network, we can represent any different configuration of metastatic disease and thus capture different organ-organ metastatic efficiencies.

To illustrate the effect of micrometastatic disease on MEIs, we compare four scenarios for a set of representative organ pairs: no micrometastases, micrometastases present in the lung, in the liver and in both locations (Figure 2). We see that Weiss’ metric differs from ours, but more importantly that the metastatic efficiency depends on the current disease state. For example, our estimate of the efficiency with which cells originating from a primary pancreatic tumor can form kidney metastases varies over six orders of magnitude, depending on whether micrometastatic lesions are present, and their location. This effect highlights an opportunity to go a step further in disease characterization than presence or absence of CTCs at staging.

The preceding analysis assumes that the filtration rate for each organ is identical for all patients in the data set. This is likely a gross oversimplification, but no clinical trial has yet determined the inpatient heterogeneity in this (currently absent) parameter set. Previously we used incidence data to calculate MEIs, but we may also reverse the process and calculate the prevalence of micrometastatic disease given incidence data and organ-pair MEIs. Under this reasoning it is possible to show, for example, that the population incidence of metastases in the adrenal gland arising from primaries in the large intestine, which equals 7.5%, can be explained not only by a single patient group composition, but by a whole collection (see online methods). Indeed, the same argument can be made for any primary-metastasis pair: the population-level data tell us nothing about a given patient.

To enable these insights and their translation to the clinic, systematic testing of individual patient filter-flow parameters is required. Measurement of CTCs at initial staging and subsequent correlation with outcomes would yield initial model parameters with which rational prospective trials could be designed. This level of understanding of an individual patient’s disease state constitutes a new type of personalized medicine, which seeks to assay not just the collection of mutations

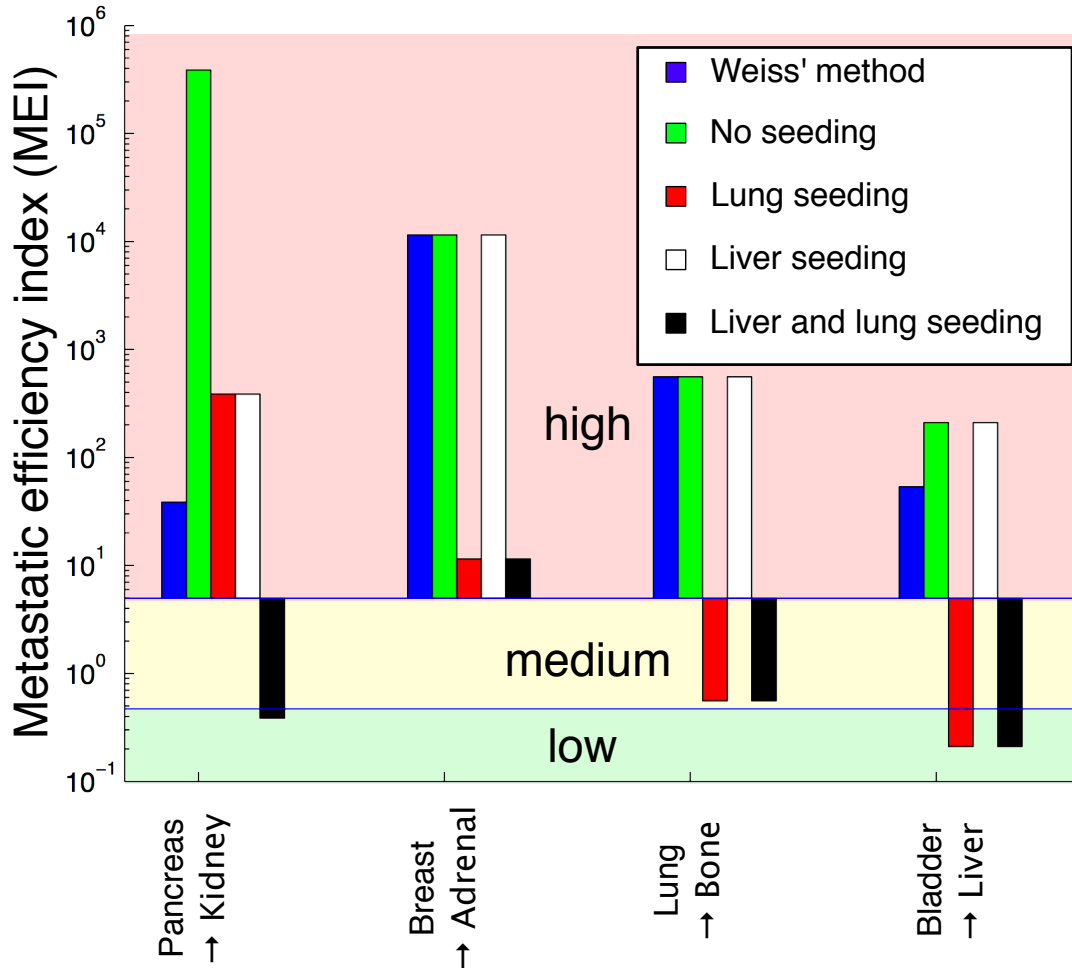


Figure 2: The impact of filter and flow characteristics on estimation of the metastatic efficient index (MEI). We have compared Weiss' original method with our filter-flow framework under the assumption of no micrometastases, micrometastases in the lung, in the liver, and in both locations. The comparison is carried out for four organ pairs that cover the canonical pathways of spread (gut \rightarrow body, body \rightarrow body, lung \rightarrow body and body \rightarrow liver). We see that because Weiss' method only considers the dynamics on the arterial side it underestimates the MEI in two of the cases (pancreas \rightarrow kidney, and bladder \rightarrow liver). From the comparison it is also evident that assumptions about the presence or absence of micrometastases heavily influences the results, in the case of pancreas \rightarrow kidney shifting the MEI six orders of magnitude from a low MEI to a high one (as defined by Weiss Weiss [1992]).

that a patient's cancer cells have accumulated, but instead their physical location. This would allow for more accurate staging and the rational inclusion of organ directed therapy in clinical trials, a

concept which is gaining popularity with recently approved methods existing for bone and liver [Harrison et al., 2013, Seront and Van den Eynde, 2012].

By further elucidating the principles underlying hematogenous metastasis, we hope to make inroads toward therapeutic strategy changes that would otherwise be impossible. Our results highlight the value of the physical perspective of the metastatic cascade, and the importance of addressing not only genetic factors, but also physiological and anatomical aspects of the process, which in this gene-centric era have been largely forgotten.

Online methods

Calculation of Metastatic Efficiency Index (MEI)

The autopsy dataset used in the analysis covers 3827 patients presenting with primary tumors in 30 different anatomical sites Disibio and French [2008]. For each primary tumor the number of metastases are reported according to anatomical site (in total 9484 metastases). As we focus on the effect of blood flow patterns, we consider only the organs for which blood flow has been measured, and this reduces the number of anatomical sites to 14 (detailed in Table 2).

For each organ-organ pair we calculate the metastatic involvement N_{ij} as the ratio between the number of occurrences of the primary tumor in organ i and the number of metastases reported in the target organ j , for each pair (i, j) presented in the autopsy data Disibio and French [2008]. We have that $0 \leq N_{ij} < 1$ and this number corresponds to the fraction of cases where a primary tumor in organ i gave rise to a metastasis in organ j . The metastatic efficiency index (MEI) from organ i to j is then defined by $M_{ij} = N_{ij}/\phi_{ij}$, where ϕ_{ij} is the relative flow of CTCs from organ i to j . This quantity takes into account the blood flow that each target organ receives (Table 1) and the reduction in CTCs that occurs en route between the two organs. For the sake of simplicity we consider only the effects of capillary bed passage, and it has been shown in clinical studies that approximately 1 in 10 000 CTCs remain viable after such a passage Okumura et al. [2009]. We thus assume that there occurs a reduction of CTC number by a factor F_k when the cells pass through organ k . As a baseline, we use the pass rate $F_k = 10^{-4}$ for all organs.

It is well known that metastases in the lung and liver have the ability to shed cells into the bloodstream and hence give rise to ‘second order’ metastases Bross et al. [1975]. If one were to measure the CTC concentration downstream of an organ containing metastases, then it would be higher than in the case of a disease-free organ. For our purposes, this implies that the presence of metastatic disease can be represented in the model as a lower reduction of CTCs in the capillary bed of the affected organ. This simplification is only valid if we disregard the biological properties of

the CTCs (since CTCs originating from metastases might have different genotypes and phenotypes compared to cells from the primary tumor), but is sufficient for our purposes. To simulate the presence of micrometastases in the lung and liver we therefore change the pass rates to $F_L = 10^{-1}$ and $F_H = 10^{-1}$ respectively.

As an example of our methodology, we now present the calculations for the MEI for breast to adrenal gland. The cancer cells leaving a breast tumor enter the circulation on the venous side and are transported via the heart to the lung capillary bed, through which only a fraction F_L pass as viable cells. These cells then flow into the arterial side of the circulation and are randomly distributed to the different organs of the body according to blood flow, of which the adrenal gland receives 0.3% (Table 1). The relative flow of CTCs from breast to adrenal gland is therefore given by $\phi_{breast,adrenal} = F_L \times 0.3 = 0.3 \times 10^{-3}$.

Patient group decomposition

Although we calculated several distinct values of MEIs depending on the pattern of metastatic spread (presence of micrometastases), it is likely that most tumors originating in the same organ have roughly the same MEI, and that the presence of metastases in the liver and lung instead affect the incidence of secondary metastases. We now show how this can be used as a means to suggest possible patient group decompositions.

The incidence, N_{ij} , relative flow of CTCs, ϕ_{ij} and the MEI, M_{ij} are related according to $M_{ij} = N_{ij}/\phi_{ij}$, or equivalently $\phi_{ij} = N_{ij}/M_{ij}$. We now assume that ϕ_{ij} is not equal for all patients, and consider four patient groups: no micrometastases, micrometastases in the lung, micrometastases in the liver and micrometastases in both. If we now let n_k denote the fraction of patients in each group, k , where $\sum n_k = 1$, then we can write

$$\sum_{k=1}^4 n_k \phi_{ij}^k = M_{ij}/N_{ij}, \quad (1)$$

where ϕ_{ij}^k is the flow of CTCs in the different patient groups. This problem is underdetermined, and the solution (in terms of the fractions n_i) is given by any point on a surface defined by (1), such that $n_i > 0$ for all patient groups and $\sum_i n_i = 1$. This implies that aggregated incidence data can be explained by many different patient group compositions, each with its distinct pattern of metastatic progression.

The population incidence of metastases in the adrenal gland arising from primaries in the large intestine equals 7.5 %, and by fixing the MEI and using the above method, the incidence rate can

be explained by a subdivision according to 25 % in the no metastasis group, 20 % in the liver metastases group, 5 % in the lung metastases group, and 50% of the patients harboring metastases in both liver and lung. However the incidence can also be explained by a subdivision of 5%, 25%, 20% and 50 % into each patient group respectively. This highlights the fact that population-based measures of incidence cannot be used to predict individual patient metastasis dynamics as different patients can exhibit fundamentally different patterns of spread.

Table 1: The relative blood flow for the organs considered, taken from Williams and Leggett [1989]. The model compartment refers to the anatomical location of the organs and their relation to the circulatory system is shown in fig. 1.

Tumor	Relative blood flow (%)	Model compartment
Liver	6.5 (arterial) + 19 (portal)	H
Lung	100	L
Adrenal	0.3	B
Bladder	0.06	B
Bone	5.0	B
Breast	1.0	B
Large intestine	4.0	G
Kidney	19.0	B
Pancreas	1.0	B
Skin	5.0	B
Small intestine	10.0	G
Stomach	1.0	G
Testes	0.05	B
Thyroid	1.5	B

Table 2: Distribution of metastases according to primary site. Data taken from Disibio and French [2008].

Primary site	No. of cases	Liver	Lung	Adrenal	Bladder	Bone	Breast	Large intestine	Kidney	Pancreas	Skin	Small intestine	Stomach	Testes	Thyroid
Liver	36	0	16	7	0	3	0	1	0	4	1	1	0	1	1
Lung	136	58	48	59	1	38	0	9	30	23	8	6	5	0	15
Adrenal	6	3	2	1	0	3	0	1	1	1	3	0	1	0	1
Bladder	183	25	30	11	0	20	0	1	9	2	1	4	0	0	1
Bone	35	6	18	4	1	15	0	1	2	3	6	0	0	0	0
Breast	432	218	247	149	17	213	54	11	40	49	124	12	17	0	35
Large intestine	560	155	101	42	10	29	0	8	20	13	9	6	1	0	8
Kidney	62	21	30	18	2	20	1	5	8	9	3	4	2	0	1
Pancreas	109	63	29	12	2	7	1	4	8	0	3	6	4	1	3
Skin	161	28	47	25	2	25	3	3	18	14	22	11	5	2	14
Small intestine	19	8	3	0	0	0	0	2	0	0	0	1	1	0	0
Stomach	477	146	84	45	7	39	2	13	14	44	11	25	3	0	5
Testes	25	19	18	6	0	8	0	2	11	3	2	3	2	1	2
Thyroid	43	10	22	4	0	6	0	0	1	3	4	1	0	0	0

Bibliography

- T.R. Ashworth. A case of cancer in which cells similar to those in the tumours were seen in the blood after death. *Australian Medical Journal*, 14(3-4):146–147, 1869.
- V Plaks, C. D Koopman, and Z Werb. Circulating tumor cells. *Science*, 341(6151):1186–1188, Sep 2013. doi: 10.1126/science.1235226.
- S. Paget. The distribution of secondary growths in cancer of the breast. 1889. *Cancer Metastasis Rev.*, 8(2):98–101, 1989.
- D.G. Rapp. In memoriam Leonard L. Weiss, Sc.D., M.D., Ph.D. *Cancer Res.*, 61:5663, 2001.
- L. Weiss. Comments on hematogenous metastatic patterns in humans as revealed by autopsy. *Clin. Exp. Metastasis*, 10(3):191–199, 1992.
- A.J. Minn, G.P. Gupta, P.M. Siegel, P.D. Bos, W. Shu, D.D. Giri, A. Viale, A.B. Olshen, W.L. Gerald, and J. Massagué. Genes that mediate breast cancer metastasis to lung. 436(7050): 518–524, 2005.
- P.D. Bos, X.H.F. Zhang, C. Nadal, W. Shu, R.R. Gomis, D.X. Nguyen, A.J. Minn, M.J. van de Vijver, W.L. Gerald, J.A. Foekens, and J. Massagué. Genes that mediate breast cancer metastasis to the brain. *Nature*, 459(7249):1005–1009, 2009.
- A. Marusyk, V. Almendro, and K. Polyak. Intra-tumour heterogeneity: a looking glass for cancer? *Nat. Rev. Cancer*, 12(5):323–34, 2012. doi: 10.1038/nrc3261.
- M. Gerlinger, A.J. Rowan, S. Horswell, J. Larkin, David Endesfelder, E. Gronroos, P. Martinez, N. Matthews, A. Stewart, P. Tarpey, I. Varela, B. Phillimore, S. Begum, N.Q. McDonald, A. Butler, D. Jones, K. Raine, C. Latimer, C.R. Santos, M. Nohadani, A.C. Eklund, B. Spencer-Dene, G. Clark, L. Pickering, G. Stamp, M. Gore, Z. Szallasi, J. Downward, P.A. Futreal, and C. Swanton. Intratumor heterogeneity and branched evolution revealed by multiregion sequencing. *N. Engl. J. Med.*, 366(10):883–92, 2012. doi: 10.1056/NEJMoa1113205.

- J.G. Scott, P. Kuhn, and A.R.A. Anderson. Unifying metastasis — integrating intravasation, circulation and end-organ colonization. *Nat. Rev. Cancer*, 12:1–2, 2012. doi: 10.1038/nrc3287. URL <http://dx.doi.org/10.1038/nrc3287>.
- J.G. Scott, D. Basanta, A.R.A. Anderson, and P. Gerlee. A mathematical model of tumour self-seeding reveals secondary metastatic deposits as drivers of primary tumour growth. *J. R. Soc. Interface*, 10:1–10, 2013.
- M. T. Milano, H. Zhang, S.K. Metcalfe, A.G. Muhs, and P. Okunieff. Oligometastatic breast cancer treated with curative-intent stereotactic body radiation therapy. *Breast Cancer Res. Treat.*, 115(3):601–8, 2009. doi: 10.1007/s10549-008-0157-4.
- M.T. Milano, A.W. Katz, H. Zhang, and P. Okunieff. Oligometastases treated with stereotactic body radiotherapy: long-term follow-up of prospective study. *Int. J. Radiat. Oncol. Biol. Phys.*, 83(3):878–86, 2012. doi: 10.1016/j.ijrobp.2011.08.036.
- R.R. Weichselbaum and S. Hellman. Oligometastases revisited. *Nat. Rev. Clin. Oncol.*, 8(6):378–82, 2011. doi: 10.1038/nrclinonc.2011.44.
- L.R. Williams and R.W. Leggett. Reference values for resting blood flow to organs of man. *Clin. Phys. Physiol. Meas.*, 10(3):187–217, 1989.
- G. Disibio and S.W. French. Metastatic patterns of cancers: results from a large autopsy study. *Arch. Pathol. Lab. Med.*, 132(6):931–939, 2008. doi: 10.1043/1543-2165(2008)132[931:MPOCRF]2.0.CO;2. URL [http://dx.doi.org/10.1043/1543-2165\(2008\)132\[931:MPOCRF\]2.0.CO;2](http://dx.doi.org/10.1043/1543-2165(2008)132[931:MPOCRF]2.0.CO;2).
- Y. Okumura, F. Tanaka, K. Yoneda, M. Hashimoto, T. Takuwa, N. Kondo, and S. Hasegawa. Circulating tumor cells in pulmonary venous blood of primary lung cancer patients. *Ann. Thorac. Surg.*, 87(6):1669–75, 2009. doi: 10.1016/j.athoracsur.2009.03.073.
- M.R. Harrison, T.Z. Wong, A.J. Armstrong, and D.J. George. Radium-223 chloride: a potential new treatment for castration-resistant prostate cancer patients with metastatic bone disease. *Cancer Manag. Res.*, 5:1–14, 2013. doi: 10.2147/CMAR.S25537.
- E. Seront and M. Van den Eynde. Liver-directed therapies: does it make sense in the current therapeutic strategy for patients with confined liver colorectal metastases? *Clin. Colorectal Cancer*, 11(3):177–84, 2012. doi: 10.1016/j.clcc.2011.12.004.
- I. Bross, W. Viadana, and J. Pickren. Do generalized metastases occur directly from the primary? *J. Chronic Dis.*, 28(3):149–159, 1975.